

## EVALUATION OF BIOACTIVITY, BIOLOGICAL AND THERMAL PROPERTIES OF SOL-GEL-DERIVED 45S5 BIOACTIVE GLASS FOR MEDICAL APPLICATIONS

\*Ali Pedram and Fathollah Moztarzadeh

Department of Biomedical Engineering, Amirkabir University of Technology, P.O. Box 15875-4413, Tehran, Iran

\*Author for Correspondence

### ABSTRACT

The 45S5 bioactive-glass is known as a material that stimulates bone-cell proliferation and form a bond to living bone tissue. In this research, the bioactivity, biocompatibility and thermal behavior of sol-gel-derived 45S5 bioglass were studied. The morphology of 45S5 bioglass sample was evaluated by scanning electron microscopy (SEM) and transmission electron microscopy (TEM). In order to investigate the bioactivity of sample, it was studied in-vitro in simulated body fluid (SBF), and their microstructure properties were examined in detail. The obtained results from X-ray powder diffraction (XRD) and Fourier transform infrared spectroscopy (FTIR) analyses showed all typical characteristic peaks of hydroxyapatite (HA) forming. The thermal behavior of 45S5 bioactive glass produced by sol-gel technique was evaluated by simultaneous thermal analysis (STA). The biological analysis of the 45S5 sample was done by cytotoxicity test and MTT cell proliferation assay. The results of biological tests showed the biocompatibility of the sol-gel-derived 45S5 bioactive glass.

**Keywords:** 45S5 Bioactive-Glass, Bioglass, Hydroxyapatite, Sol-Gel Technique, Biocompatibility

### INTRODUCTION

Ceramics in different types and shapes are used to make implants which have many industrial and orthopedic applications due to desirable electric, mechanical and biological properties and are now commonly used in the medical fields as dental and bone implants (Mozafari *et al.*, 2010; Mening *et al.*, 1998). Bioactive glasses are a subclass of bioactive ceramics that their composition is consists of silicon, sodium, potassium, calcium, phosphorous and magnesium oxides, which can be derived by different techniques such as sol-gel and melting. Bioactive ceramics increase the probability of formation of HA (inorganic component of natural bone) on the surface of biomaterials (Ding *et al.*, 2010; Boccaccini *et al.*, 2006; Gallardo *et al.*, 2001; Santos *et al.*, 1999; Innocenzi *et al.*, 1992) such as 304 and 316L stainless steels (Naghib *et al.*, 2012; Naghib *et al.*, 2012). Hench (1982) reported the first bioactive glass that is known as 45S5 and with the composition of (wt.%) 45% SiO<sub>2</sub>, 24.5% Na<sub>2</sub>O, 24.5% CaO and 6% P<sub>2</sub>O<sub>5</sub>. 45S5 bioactive-glass can be prepared via sol-gel and melting techniques, which may have enough potential to be biomaterials for human body due to their bioactivity and biocompatibility. 45S5 bioglass has reputation for having the potential of bone mineralization and biocompatibility (Vargas *et al.*, 2009). There are significant advantages for a sol-gel-derived glass which are very important for biomedical applications. These glasses can improve the purity and homogeneity that is required for optimal bioactivity because of low processing temperatures (600-700 °C). They can also interconnect the porosities in nanometer scale that can be varied to control dissolution kinetics or be impregnated with biologically active phases such as growth factors.

In the present research, an investigation of biological (in-vivo performance) and thermal properties of sol-gel-derived 45S5 bioactive glass for biomedical applications was undertaken. For this aim, the 45S5 bioglass powder was prepared by sol-gel technique and microstructure, biological properties and thermal behavior were characterized. Then, the powder of 45S5 bioglass immersed in simulated body fluid (SBF) at 37 °C for 14 days and formation of HA (hydroxyapatite) layer was evaluated by X-Ray diffraction (XRD) and Fourier transform infrared (FTIR) techniques. The ability of the constructs to support the attachment and growth of osteoblastic cells was evaluated. In the previous *in-vitro* investigations of

**Research Article**

biomaterials for bone repair and tissue engineering, different types of cell line were been chosen (Foppiano *et al.*, 2004; Inoue *et al.*, 2004). In this research, The SAOS-2 (Sarcoma osteogenic) cell line was chosen for the experiments. Also, the cytotoxicity of 45S5 bioglass powder was done by the cytotoxicity test in comparison with control sample.

**MATERIALS AND METHODS**

**Synthesis of 45S5 Bioactive-Glass via Sol–Gel Technique**

Table 1 gives information about the chemical composition of 45S5 bioactive glass. In order to synthesize 1 mole 45S5 bioglass by sol-gel technique, 102.88 cm<sup>3</sup> of tetraethoxysilane (TEOS) was added to 50 cm<sup>3</sup> of 0.1 M nitric acid, and then placed on a stirrer for performing the hydrolysis process. At this stage, nitric acid was used as the sol environment and TEOS was utilized as a source of SiO<sub>2</sub> supply. Then, 8.861 cm<sup>3</sup> of triethylphosphate (TEP) was added to the system as the P<sub>2</sub>O<sub>5</sub> supply, which was then stirred for 1 hour. Then 63.52 g of calcium nitrate tetrahydrate powder was added to the system, which was previously solved in distilled water as the CaO supply, and again a one hour period of stirring.

The process was continued by last stage that was adding 25.864 g of sodium carbonate (as Na<sub>2</sub>O supply, previously solved in distilled water) and placing the whole system on a stirrer for 2 hours for completing the process of hydrolysis reactions. The molar ratio of water to TEOS (H<sub>2</sub>O:TEOS) was chosen as equal to 12:1.

The obtained sol was put in an oven for 8 hours at 60 °C, in order to reach to the gel state and become suitable for next experiments.

**Table 1: Chemical Composition of 45S5 Bioactive-Glass (in Mole and Weight Percent)**

	SiO <sub>2</sub>	CaO	Na <sub>2</sub> O	P <sub>2</sub> O <sub>5</sub>
Mol %	46.1	26.9	24.4	2.6
Wt %	45	24.5	24.5	6

**Preparation of SBF Solution**

The SBF solution was prepared by dissolving reagent-grade NaCl, KCl, NaHCO<sub>3</sub>, MgCl<sub>2</sub>·6H<sub>2</sub>O, CaCl<sub>2</sub> and KH<sub>2</sub>PO<sub>4</sub> into distilled water and buffered at pH=7.3 with TRIS (trishydroxymethyl aminomethane) and HCl 1N at 37 °C. The composition of prepared SBF solution is given in Table 2, compared with the human blood plasma.

**Table 2: Ion Concentrations of Simulated Body Fluid (SBF) in Comparison with Human Blood Plasma**

Ions	Plasma (mmol/l)	SBF (mmol/l)
Na <sup>+</sup>	142.0	142.0
K <sup>+</sup>	5.0	5.0
Mg <sup>+</sup>	1.5	1.5
Ca <sup>+</sup>	2.5	2.5
Cl <sup>-</sup>	103.0	103.0
HCO <sub>3</sub> <sup>-</sup>	27	27
HPO <sub>4</sub> <sup>2-</sup>	1.0	1.0
SO <sub>4</sub> <sup>2-</sup>	0.5	0.5

**Characterization**

**XRD Analysis**

XRD analysis (Philips X'Pert-MPD system with a Cu Kα wavelength of 1.5418 Å) was used to analyze the crystal structure and phase present in the samples after immersing in SBF. The diffractometry was operated at 40 kV and 30 mA at the 2θ range of 20–55° employing a step size of 0.02°/s.

## Research Article

### FTIR Analysis

FTIR analysis (Bomem, MB-100) was used to observe functional groups developed in the specimens and specially investigated the formation of apatite layer on the surface of 304 SS coated by 45S5 bioactive-glass which was immersed in SBF at 37 °C for 14 days. The FTIR spectra were investigated in the 400–4000  $\text{cm}^{-1}$  range.

### SEM and TEM Observations

SEM analysis (Phillips XL 30) and TEM analysis (Philips EM208) was used to observe the structure and morphology of the 45S5 bioactive-glass powder produced by sol-gel technique.

### Thermal Analysis

The thermal analysis (STA 1640, 10 deg./min, 25-1000 °C) of sol-gel-derived 45S5 bioactive glass sample was evaluated by simultaneous thermal analysis (STA) to determine the temperature of hydroxyl group loss and powder decomposition.

### Biological Evaluations

Investigating the bioactivity of the 45S5 bioactive-glass was performed by imprisoning in SBF solution in an incubator at 37 °C for 14 days. They were then brought out from the incubator and desiccated at room temperature. Also, the biological analysis of the 45S5 sample was performed by cytotoxicity test and MTT cell proliferation assay. The cytotoxicity test was performed and the images of the results of the test in comparison with control sample after 48 hours culturing the 45S5 sample was taken with optical microscope. The culture media of MTT cell proliferation assay was SAOS-2 cells (cancer class of bone cells) and the test was performed for the period of 1-7 days.

## RESULTS AND DISCUSSION

### Crystal Structure and Bioactivity

The XRD patterns of sol-gel-derived 45S5 bioactive glass before and after 14 days of immersion in SBF solution are shown in Figure 1. In the untreated pattern of the sample, it almost took an amorphous state indicative of the internal disorder and glassy nature of material and it is worth mentioning that the sample did not show any crystalline states as shown in Figure 1(a). As it can be seen in Figure 1(b) for sol-gel-derived 45S5 bioglass sample after immersion in SBF solution, the XRD results indicated the formation of HA on the sample according to 26° and 32° peaks that are assigned to be (211) and (002) planes of apatite crystals referring to the standard JCPDS cards (No. 09-0432). According to Figure 1(b), it is significant to mention that for the sol-gel-derived sample after immersion in SBF, the other peaks of apatite at 39°, 46° and 56° appeared that may confirm the formation of the apatite phase.

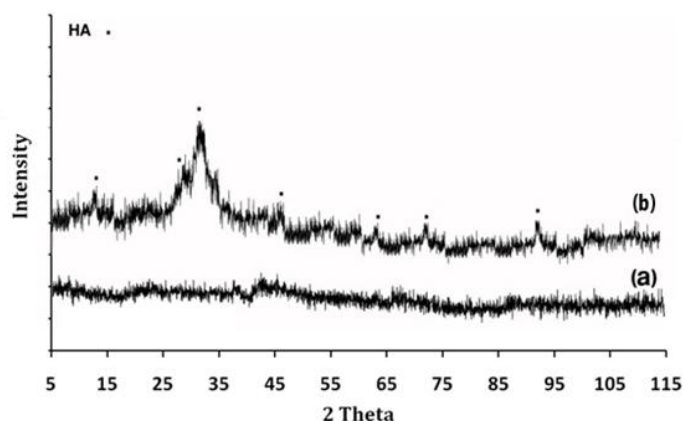


**Figure 1: XRD Patterns of the Sol-Gel-Derived 45S5 Bioactive-Glass Sample (a) before and (b) after 14 Days of Immersion in SBF Solution**

The formation of HA layers was also confirmed by FTIR analysis, which is presented in Figure 2. After 14 days of immersing the 45S4 bioactive glass specimen in SBF solution, the FTIR spectroscopy patterns

### Research Article

of sample showed large peaks at the wave number range of  $1000\text{--}1200\text{ cm}^{-1}$ , which proved the formation of an amorphous rich-layer of CaO and  $\text{P}_2\text{O}_5$ . Moreover, a peak related to P–O bond was observed at the wave number range of  $500\text{--}600\text{ cm}^{-1}$ , which showed the formation of HA layer on the sample (Onishi *et al.*, 1997). The obtained peaks at the range of  $3400\text{--}3500\text{ cm}^{-1}$  were associated to the absorbed water in the system. As it can be seen in Figure 2(b) for the sol–gel-derived sample, the intensities of bands associated to phosphate group vibrations increased and the spectrum became quite similar to that of HA. The characteristic bonds exhibited in the sample's spectra assigned here are the following: Two bonds were observed at  $3460$  and  $673\text{ cm}^{-1}$  due to the stretching mode of hydrogen-bonded  $\text{OH}^-$  ions and liberational mode of hydrogen-bonded  $\text{OH}^-$  ions, respectively. The bond at  $1131\text{ cm}^{-1}$  arises from  $\nu_3\text{ PO}_4$  and the bond at  $604$  arises from  $\nu_4\text{ PO}_4$  (Mozafari *et al.*, 2010; Hamlekhan *et al.*, 2010).

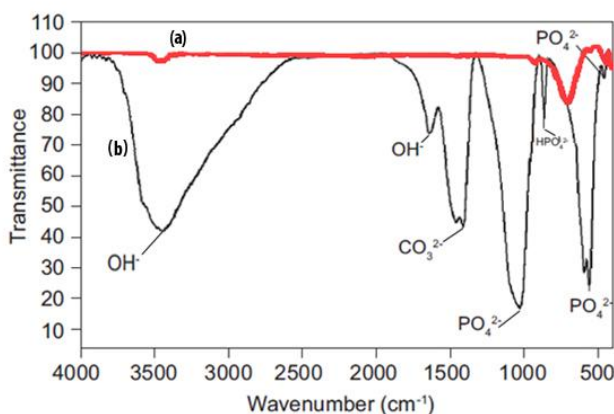


**Figure 2: FTIR Spectra of the Sol–Gel-Derived 45S5 Bioactive-Glass Sample (a) before and (b) after 14 Days of Immersion in SBF**

### SEM and TEM Observations

SEM observations were used for evaluating the morphology and microstructure of the specimens before and after immersion in SBF solution. As it can be seen in Figure 3(a), before immersion in SBF, the SEM micrograph showed a distribution of small particles and enormous agglomerated particles that were composition of small particles that had been joined physically. Also, SEM image of 45S5 bioactive glass produces by sol-gel technique after 14 days of immersion in SBF is presented in Figure 3(b).

TEM observations were used to evaluate the morphology, microstructure and the size of crystallites as shown in figure 4(a). The length of crystallites was  $38\pm 10\text{ nm}$  and their width was  $12\pm 5\text{ nm}$ . The difference in the speed of stirring of the solution was the most synthesis parameter that could cause the difference in the crystallites size. The crystallites size was a nano and rod-shape, however, as it can be seen in figure 3(b), there was an accumulation of particles that had been joined together.

### Thermal Analysis

Figure 5 shows the thermal analysis of sol-gel-derived 45S5 bioactive glass sample was performed by simultaneous thermal analysis (STA). The analyzed sample of 45S5 bioactive glass showed two levels of weight deduction: (a) in the temperature range of  $25\text{--}200\text{ }^\circ\text{C}$  that was due to loss in adsorbed physical water in the sample, (b) in the temperature range of  $650\text{--}750\text{ }^\circ\text{C}$  that was because of dehydroxylation of the sample.

### Biological Analysis

Cytotoxicity test and MTT cell proliferation assay were used to evaluate the biological analysis of sol-gel-derived 45S5 bioactive glass. In the cytotoxicity test, the optical microscopy images of the samples (control and 45S5 bioglass) after 48 hours culturing were taken. Figure 6(a) shows the optical microscopy images of the control and figure 6(b) shows the optical microscopy image of 45S5 bioactive glass. As it can be seen by comparison of this images, there was a layer of spindle–shape fibroblast cells on the sample of sol-gel-derived 45S5 bioactive glass that cell line spreading and the morphology of cells is

**Research Article**

shown the compatibility of the powder sample of 45S5 bioglass produced by sol-gel technique. The spherical bodies are dead cells, however, the death of this cell was not due to their toxicity, but it was because of lack of space and the nutrition required for their growth. In addition, for evaluating the cell toxicity and cell proliferation, the MTT assay was done. The test performed in the period of 1-7 days and the results are shown in figure 7. Overall, the cell density went up sharply and peaked at 5 days and showed the biocompatibility of the sol-gel-derived 45S5 bioactive glass. Then, the amount of adhered cells to the sample went down slightly and had a constant trend.

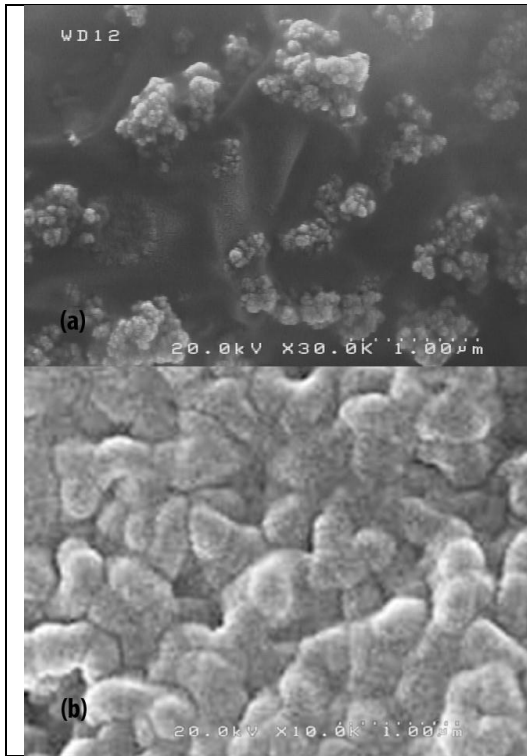


**Figure 3: SEM Micrograph of the Sol-Gel-Derived 45S5 Bioactive-Glass Sample (a) before and (b) after 14 Days of Immersion in SBF Solution**

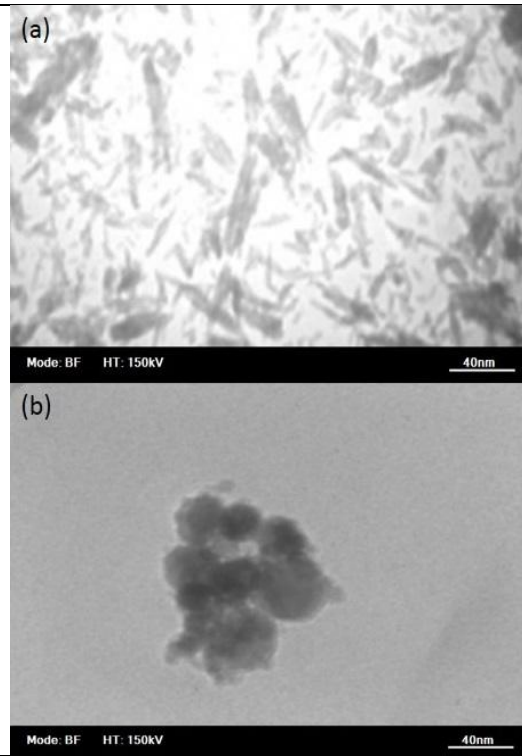


**Figure 4: TEM Micrograph of the Sol-Gel-Derived 45S5 Bioactive-Glass Sample**

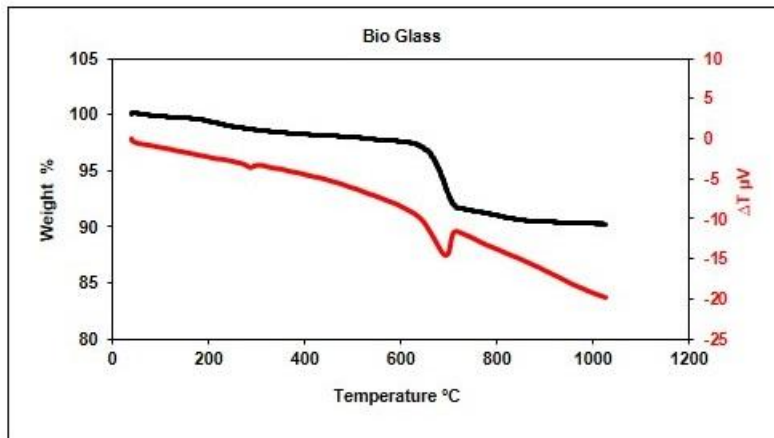


**Figure 5: The Simultaneous Thermal Analysis (STA) Pattern of Sol-Gel Derived 45S5 Bioactive Glass**

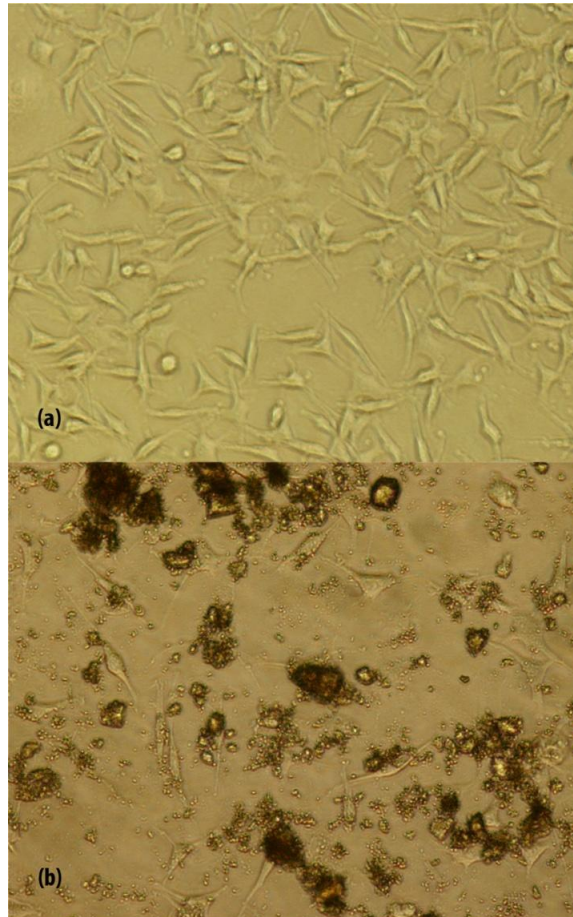


**Figure 6: The Optical Microscopy Images of Cytotoxicity Test (a) Control (b) Sol-Gel-Derived 45S5 Bioactive Glass**

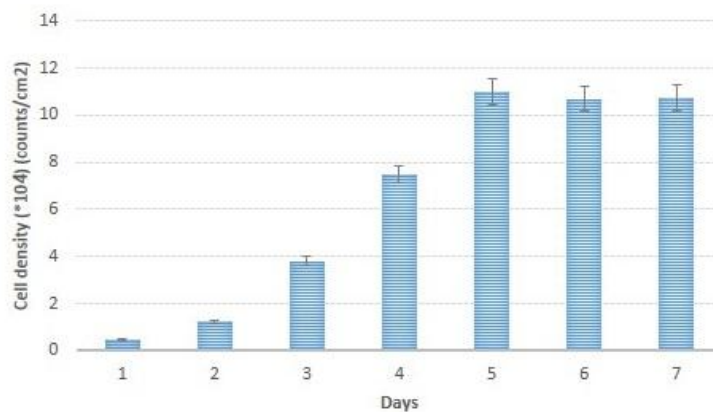


**Figure 7: The Results of MTT Cell Proliferation Test with SAOS-2 Cells for 1-7 Days**

### **Conclusion**

The comparison of results of XRD, FTIR and SEM analysis in this research proved that the sol-gel-derived 45S5 bioactive glass had a suitable bioactivity after 14 days of immersion in SBF and formation of HA layer on the samples proved with all typical characteristic peaks of hydroxyapatite. In addition, the results of biological analysis (cytotoxicity test and MTT cell proliferation assay) in this research revealed

### Research Article

that the 45S5 bioactive glass had a sufficient biocompatibility for medical applications. Also, two stages of decreasing in the weight of the 45S5 bioglass illustrated in the thermal simultaneous thermal analysis of the sample that were in the temperature ranges of 25-200 °C and 650-750 °C that were because of loss in adsorbed physical water and dehydroxylation of the sample, respectively.

### ACKNOWLEDGEMENT

This research was supported by the School of Biomedical Engineering at Amirkabir University of Technology, and they are gratefully acknowledged.

### REFERENCES

- Boccaccini AR, Peters C, Roether JA, Eifler D, Misra SK and Minay EJ (2006).** Electrophoretic deposition of polyetheretherketone (PEEK) and PEEK/bioglass coatings on NiTi shape memory alloy wires. *Journal of Materials Science* **41** 8152-8159.
- Krause D, Thomas B, Leinenbach C, Eifler D, Minaya EJ and Boccaccini AR (2006).** The Electrophoretic deposition of bioglass particles on stainless steel and Nitinol substrates. *Surface and Coatings Technology* **200**(16-17) 4835.
- Ding MH, Wang BL, Li L and Zheng YF (2010).** Preparation and characterization of TaC<sub>x</sub>N<sub>1-x</sub> coatings on biomedical 316L stainless steel. *Surface and Coatings Technology* **204**(16-17) 2519.
- Foppiano S, Marshall SJ, Marshall GW, Saiz E and Tomsia AP (2004).** The influence of novel bioactive glasses on in vitro osteoblast behavior. *Journal of Biomedical Materials Research Part A* **71A** 242–9.
- Gallardo J, Galliano P and Duran A (2001).** Bioactive and Protective Sol-Gel Coatings on Metals for Orthopaedic Prostheses. *Journal of Sol-Gel Science and Technology* **21**(1-2) 65.
- Hamlekhan A, Mozafari M, Nezafati N, Azami M and Hadipour H (2010).** A proposed fabrication method of novel PCL-GEL-HAp nanocomposite scaffolds for bone tissue engineering applications. *Advanced Composites Letters* **19**(4) 123–130.
- Hench LL (1982).** *CRC Handbook of Bioactive Ceramics*, **1**, (CRC Press, Boca Raton, Florida, USA).
- Hench LL and Wilson J (1984).** Surface-active biomaterials. *Science* **226** 630.
- Innocenzi PC, Guglielmi M, Gobbin M and Colombo P (1992).** Coating of metals by the sol-gel dip-coating method. *Journal of the European Ceramic Society* **10** 431.
- Inoue M, LeGeros RZ, Inoue M, Tsujigiwa H and Nagatsuka H (2004).** In vitro response of osteoblast-like and odontoblast-like cells to unsubstituted and substituted apatites. *Journal of Biomedical Materials Research Part A* **70A** 585–93.
- LeGreros Z (1993).** Biodegradation and Bioresorption of Calcium Phosphate Ceramics. *Clinical Materials* **14** 65-88.
- Mening M, Schelle C, Durán A, Damborenea JJ, Guglielmi M and Brusatin G (1998).** Investigation of Glass-Like Sol-Gel Coatings for Corrosion Protection of Stainless Steel Against Liquid and Gaseous Attack. *Journal of Sol-Gel Science and Technology* **13**(1-3) 717.
- Mozafari M, Moztarzadeh F and Tahriri M (2010).** Investigation of the physico-chemical reactivity of a mesoporous bioactive SiO<sub>2</sub>-CaO-P<sub>2</sub>O<sub>5</sub> glass in simulated body fluid. *Journal of Non-Crystalline Solids* **356** 1470.
- Mozafari M, Moztarzadeh F, Rabiee M, Azami M, Tahriri M, Moztarzadeh Z and Nezafati N (2010).** Development of macroporous nanocomposite scaffolds of gelatin/bioactive glass prepared through layer solvent casting combined with lamination technique for bone tissue engineering. *Ceramics International* **36**(8) 2431–2439.
- Mozafari M, Rabiee M, Moztarzadeh F, Azami M and Maleknia S (2010).** Biomimetic formation of apatite on the surface of porous gelatin/bioactive glass nanocomposite scaffolds. *Applied Surface Science* **257** 1740–1749.

**Research Article**

- Naghib SM, Ansari M, Pedram A, Moztarzadeh F, Feizpour A and Mozafari M (2012).** Bioactivation of 304 Stainless Steel Surface through 45S5 Bioglass Coating for Biomedical Applications. *International Journal of Electrochemical Science* **7** 2890 – 2903.
- Naghib SM, Pedram A, Ansari M and Moztarzadeh F (2012).** Development and Characterization of 316 L Stainless Steel Coated by Melt-derived and Sol-gel derived 45S5 Bioglass for orthopedic applications. *Ceramics – Silikáty* **56**(1) 89-93.
- Onishi HO, Kutrshtani S, Yasukawa E, Iwaki H, Hench LL, Wilson J, Tsuji E and Sugihara T (1997).** Particulate bioglass compared with hydroxyapatite as a bone graft substitute. *Clinical Orthopaedics and Related Research* **334** 316.
- Santos EM, Radin S and Ducheyne P (1999).** Sol-gel derived carrier for the controlled release of proteins. *Biomaterials* **20** 1695.
- Uchida M, Kim HM and Kukubo T (2002).** Structural dependence of apatite formation on zirconia gels in a simulated body fluid. *Journal of the Ceramic Society of Japan* **110** 710-715.
- Vargas GE et al., (2009).** Biocompatibility and bone mineralization potential of 45S5 Bioglass®-derived glass–ceramic scaffolds in chick embryos. *Acta Biomaterialia* **5**(1) 374–380.